Classification of trabecular patterns in the proximal femur using the vector representation algorithm: its correlation to the degree of osteoporosis

M. Pecelis[1], J. Massa[2], L. Favro Velo[3], M. Santiago[3,4] and E. Caselli[3,5]

[1] Centro de Diagnóstico por Imágenes, 7000 Tandil, Argentina
[2] INTIA Universidad Nacional del Centro, 7000 Tandil, Argentina
[3] IFAS, Universidad Nacional del Centro, 7000 Tandil, Argentina
[4] Consejo Nacional de Investigaciones Científicas y Técnicas (CONICET), Buenos Aires, Argentina
[5] Comisión de Investigaciones Científicas de la Provincia de Buenos Aires, 1900 La Plata, Argentina

Abstract— **The vector representation algorithm (VRA) has been employed for classifying textures of two regions of the proximal femur, i.e., the Ward's triangle (WT) and the principal compressive group (PCG), in order to assess whether it is appropriate to discriminate changes in trabecular textures of healthy, osteopenic and osteoporotic patients.**

Keywords— **Osteoporosis, texture analysis, computer aided diagnosis.**

I. Introduction

Normal bone consists of a cortical shell enclosing trabecular tissue. Osteoporosis is characterized by a loss of bone mass and a deterioration of the trabecular structure (loss of trabecular plates and of their connection). Mass loss is usually measured by means of dual energy X-ray absorptiometry (DXA), which gives an estimation of the bone mineral density (BMD). Another exam for evaluating the presence of osteoporosis relies on measuring the velocity and attenuation of ultrasound waves in trabecular tissues. Quantitative computed tomography (QCT) is another exam to estimate the mass loss [1]. Although BMD is an indicator of bone strength it alone cannot predict the risk of osteoporotic fracture [2]. Now it is widely accepted that characterization of the texture of trabeculae could be a complement to BMD exams in order to improve the prediction of fractures brought about by osteoporosis [3].

The main imaging techniques employed for characterizing the structure of trabecular tissues are peripherical quantitative computed tomography (pQCT) [4], magnetic resonance imaging (MRI) [1] and X-ray pictures [5]. Both pQCT and MRI produce 3D images of trabecular tissue, but their application is limited by their cost and availability. Veenland et al. have shown that texture analysis of radiographs is suited to characterize trabecular bone architecture [6]. Trabecular structures have been analyzed employing different algorithms, such as fractals, Fourier transform, wavelets, Gabor filter, Laws' masks among others [2,7-9].

In this paper we report the results of investigations on the performance of the vector representation algorithm for discriminating changes in texture of trabecular tissues due to osteoporosis.

II. Vector representation algorithm

The vector representation algorithm has been successfully employed in analytical chemistry for analyzing spectra [10-11]. Recently Skopec et al. used the VRA for classifying glow curves yielded by thermoluminescent detectors exposed to proton, photon and proton-photon radiation [12].

The VRA is quite simple. It compares two set of values in order to find out whether they are identical, and if they differ, gives a number which is a measure of the differences between them. The set of values are considered as being vectors and must have the same dimension. The inner product of both vectors, say ***A*** and ***B***, divided by their modulii, i.e.:

$$\frac{A \bullet B}{|A||B|} = \cos(\alpha)$$

where α is the angle between both N-dimensional vectors. If they are identical then $\cos(\alpha) = 1$.

This algorithm can be used to characterize the texture of an image as follows. Let us consider a region of interest (ROI) of an image, for example, the Ward's triangle in the proximal femur. The ROI is chosen to be a square, say, of $(N+1) \times (N+1)$ pixels. The gray level corresponding to the pixel (i,j) is indicated with $I_{j,k}$. Each row can be considered as a vector of length $(N+1)$. By multiplying a given row, say, the i-row, by the vector whose components are all 1's one obtains:

$$\cos(\alpha_i) = \frac{\sum_{j=0}^{N} I_{i,j}}{\sqrt{\sum_{j=0}^{N} I_{i,j}^{\,2}}\sqrt{N+1}}$$

Thus $\cos(\alpha_i)$ is a measure of the non-uniformity of the intensity of the pixels located in the *i*-row. This calculation is made for each row and the average value, i.e.

$$\frac{\sum_{i=0}^{N}\cos(\alpha_i)}{N+1} = f1$$

is computed. This procedure is also performed for the columns and the pixel vectors parallel to both diagonals, as shown in Fig. 1. Thus the anisotropy of a texture will be reflected in the four values *f*1, *f*2, *f*3 and *f*4. Note that for calculating *f*3 and *f*4 the length of the vectors varies with the index *i*.

The rationale behind analyzing the asymmetry of textures is that osteoporosis causes an increment of the texture asymmetry [13]. Lemineur et al. determined the anisotropy of the calcaneus by means of a method dubbed Directional Average, which relies on the Anisotropic Fractional Brownian Field [14]. They found that the textures of the osteoporotic patients were more anisotropic than the group of healthy patients.

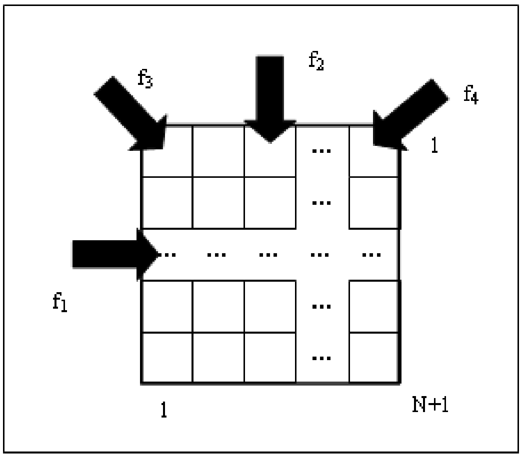

Fig. 1 Directions of the anisotropy values

III. Materials and methods

Antero-posterior femur radiographs corresponding to 120 patients were digitized by means of a Radlink Laser Pro 16 digitizer with a resolution of 0.26mm×0.26mm. This resolution is satisfactory since the average distance among trabeculae ranges from 0.3 to 0.5 mm. Later the pictures were filtered with a high-pass filter in order to increase the trabecular contribution to the X-ray picture [9]. The employed filter removed low frequency components by using a gaussian averaging of the neighborhood.

A radiologist (M Pecelis) selected two ROI's from each picture, i.e., a ROI in the WT and another in PCG. For each region *f*1, *f*2, *f*3 and *f*4 were calculated. In order to get an indicator of the anisotropy of each ROI texture the angles between vectors (*f*1,*f*2,*f*3,*f*4) and (1,1,1,1), denoted in what follows with ACos, were computed.

Finally, the calculated ACos anisotropy indexes of each patient were plotted against the corresponding T-score values measured with a Sunlight Omnisense ultrasound equipment.

IV. Results

The scatter plots for WT and PCG are shown in Fig. 2(a) and Fig. 2(b) respectively. Comparison of figures 2(a) and 2(b) shows that for healthy people (T-score > –1) the differences between the ACos values for the WT and the PCG are no significant, i.e., most values are located between 0 and 0.1. Thus the texture of trabecular tissues in healthy people is highly symmetrical. For osteopenia the ACos values extend from 0 to nearly 0.2 in the PCG, while the values range from 0.12 to 0.22 in the WT. This result indicates that in osteopenic patients the trabecular texture changes first in the WT by losing symmetry, what is in agreement with the finding that the PCG is the last region of the proximal femur which is affected by osteoporosis [15].

For people having osteoporosis the ACos values range mainly from 0 to 0.1 in the PCG, a range similar to that of healthy patients, again a result indicating that the PCG is the region less affected by osteoporosis. On the contrary, the ACos values in the WT are scattered between 0.05 and 0.4. Further, the changes in the anisotropy of textures in WT correlates with the degree of osteoporosis, T-score, measured with ultrasound (Pearson's correlation coefficient $r = -0.633$).

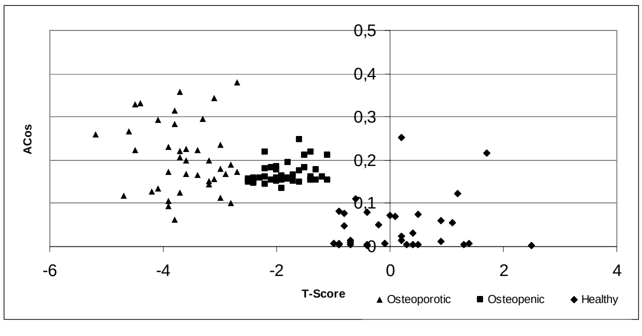

Fig. 2 (a) ACos values for WT

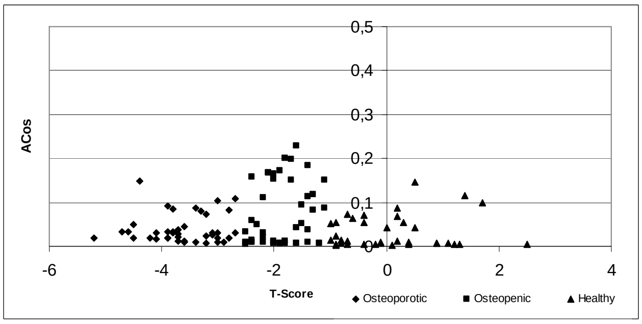

Fig. 2 (b) ACos values for PCG

V. Conclusions

The results show that osteoporosis reduces the symmetry of trabecular tissues in the proximal femur, significantly in the WT and very little in the PCG. The index ACos, which is the measure of asymmetry given by the VRA, correlates satisfactory with T-scores obtained from ultrasound. Therefore the analysis of trabecular textures with the VRA is an appropriate index to be employed with other ones, such as BMD, ultrasound, etc., in the analysis of the risk of fractures due to osteoporosis.

References

1. Lang T, Augat P, Majundar S et al. (1998) Non invasive assessment of bone density and structure using computed tomography and magnetic resonance. Bone 22 (5) pp 149S-153S
2. Lin J C, Grampp S, Kothari L et al. (1999) Fractal analysis of proximal femur radiographs: Correlation with biomechanical properties and bone mineral density. Osteoporosis Int. 9, pp 516-524
3. Karunanithi R, Ganesan S, Panicker T M R et al. (2007) Assessment of bone mineral density by DXA and the micro-architecture of the calcaneum by texture analysis in pre- and post-menopausal women in the evaluation of osteoporosis. J. Med. Phys. 32 (4) pp 161-168
4. Mueller T L, Stauber M, Kohler et al. (2009) Non-invasive bone competence analysis by high-resolution pQCT: An in vitro reproducibility study on structural and mechanical properties at the human radius. Bone 44 (2) pp 364-371
5. Apostol L, Boudousq V, Basset O et al. (2006) Relevance of 2D radiographic texture analysis for assessment of 3D bone micro-architecture. Med. Phys. 33, 9 (2003), pp 541–548
6. Veenland J F, Grashuis J L, Weinans H et al. (2002) Suitability of texture features to assess changes in trabecular bone architecture. Pattern Recogn. Lett. 23, pp 395-403
7. Faber T D, Yoon D C, Service S K et al. Fourier and wavelets analysis of dental radiographs detect trabecular changes in osteoporosis. Bone 35 pp 403-411
8. Pramudito J T, Soegijoto S, Mengko T R et al. (2007) Trabecular pattern analysis of proximal femur radiographs for osteoporosis detection. J. Biomed. Pharm. Eng. 1:1 pp 45-51
9. Rachidi M, Marchadier A, Gadois C et al. (2008) Laws's masks descriptors applied to bone texture analysis: an innovative and discriminant tool in osteoporosis. Skeletal Radiol. 37 pp 541-548
10. Stein S E and Scott D R (1994) Optimization and testing of mass spectra library search algorithms for compound identification. J. Am. Soc. Mass Spectr. 5, pp 859-866
11. Wan K X, Vidavsky I and Gross L (2002) Comparing similar spectra: from similarity index to spectral contrast angle. J. Am. Soc. Mass Spectr. 13, pp 85-88
12. Skopec M, Loew M, Price J et al. (2008) Classification of mixed-radiation fields using the vector representation of thermoluminiscent glow curves. Radiat. Meas. 43 pp 410-413
13. Sugita H, Oka M, Toguchida J et al. (1999) Anisotropy of osteporotic cancellous bone. Bone 24(5) pp 513-516
14. Lemineur G, Harba R, Jennane R et al. (2004) Fractal anisotropy measurements of bone texture radiographs. First Int. Symp. on Control, Communications and Signal Processing, March 21-24 2004, Hammamat Tunisia
15. Singh M, Nagrath A R and Maini P S, (1970) Changes in trabecular pattern of the upper end of the femur as an index of osteoporosis. J. Bone Joint Surg. Am. 52 pp 457-467